



DOI: 10.32768/abc.202183216-225

Assessment of Tumor Cell Death After Percutaneous Ultrasound–Guided Radiofrequency Ablation of Breast Carcinoma: A Prospective Study

Anna Gumà^a, Teresa Soler^b, César G. Chappuis^c, Alazne Valdivielso^a, Anna Petit^b, Maria J. Pla^d, Catalina Faló^e, Sònia Pernas^e, Raúl Ortega^e, Laia Pérez^a, María Vicente^a, Eulalia Fernández-Montoli^d, Miriam Campos^d, Fernando Burdio^f, Jordi Ponce^d, Nahum Calvo^a, Amparo García-Tejedor^d

^a Department of Radiology, Hospital Universitari de Bellvitge, Hospitalet de Llobregat, Barcelona, Spain

^b Department of Pathology, Hospital Universitari de Bellvitge, Hospitalet de Llobregat, Barcelona, Spain

^c Department of Pathology, Consorci del Laboratori Intercomarcal de l'Alt Penedès, l'Añoia i el Garraf. Sant Pere de Ribes, Barcelona, Spain

^d Department of Gynaecology, Hospital Universitari de Bellvitge, Hospitalet de Llobregat, Barcelona, Spain

^e Department of Oncology, Institut Català d'Oncologia, Hospitalet de Llobregat, Barcelona, Spain

^f Department of Surgery, Parc de Salut-Hospital del Mar, Barcelona, Spain

ARTICLE INFO

Received:
06 March 2021
Revised:
26 April 2021
Accepted:
29 April 2021

Key words:

Early breast cancer,
radiofrequency ablation,
ultrasound,
NADH-diaphorase staining,
cytokeratins.

ABSTRACT

Background: Current trends in breast cancer treatment include the use of less aggressive surgeries to reduce morbidity, shorten hospital stays and improve cosmetic results. The aim of the study is to assess tumor cell viability after percutaneous ultrasound (US)-guided radiofrequency ablation (RFA) for small breast cancer by a combination of staining techniques.

Methods: A prospective study was conducted at a single institution from 2013 to 2017. Twenty women with invasive ductal carcinoma of the breast measuring ≤ 20 mm were treated with US-guided RFA followed immediately by surgical resection. Tumor viability pre- and post-RFA was assessed with Hematoxylin and Eosin (H&E), Nicotinamide adenine dinucleotide (NADH), Succinate dehydrogenase (SDH), Cytochrome c oxidase (COX), Terminal deoxynucleotidyl transferase dUTP nick end labeling (TUNEL) and Cytokeratin 18 and 19 (CK18/CK19) staining techniques. Outcomes and correlation with the different techniques were evaluated with principal component analysis Cronbach's alpha.

Results: Oxidative enzymes in frozen sections showed loss of SDH and NADH in 13 of the 16 tumors (81%) and COX in 11 of the 13 tumors (84%). In paraffin-embedded tissues, CK18 was negative or markedly reduced in 98% and CK19 in 100% of the cases. Lack of evidence of cell death was seen in 3 cases where the maximum temperature achieved at the center of the tumor was $\leq 70^\circ\text{C}$. The reliability and internal consistency between the different staining techniques was high (Cronbach's alpha, 0.8), with concordance between the staining results of the oxidative enzymes and of CK18/CK19.

Conclusion: Loss of tumor viability in small breast tumors after US-guided percutaneous RFA could be assessed in our series with different staining methods. CK18 and CK19 could be used in paraffin-embedded tissues as surrogate markers of tumor cell viability after immediate RFA.

*Address for correspondence:

Anna Gumà, MD
Address: Department of Radiology, Hospital Universitari de Bellvitge, Hospitalet de Llobregat, Carrer de la Feixa Llarga, s/n 08907 Hospitalet de Llobregat, Barcelona, Spain.
Email: anna.guma@bellvitgehospital.cat

Introduction

Current trends in breast cancer treatment include the use of less aggressive surgeries to reduce morbidity, shorten hospital stays and improve cosmetic results. Several percutaneous ablation



techniques have been studied, such as cryoablation, laser ablation, microwave irradiation, high-intensity focused ultrasound, electroporation and radiofrequency ablation (RFA).^{1,2} RFA is one of the most promising techniques for the treatment of small breast cancers, with a high but variable success rate of complete ablation ranging from 77 to 100%.¹⁻⁵

During an RFA, a needle is inserted into the middle of the tumor to induce tissue electrocoagulation, creating an ellipsoid region of necrotic tissue that aligns with the tip of the needle electrode.^{5,6} Since Jeffrey et al. first introduced RFA for breast cancer treatment in 1999⁷, several electrodes have been used. Analysis of the tumor specimen after an RFA can be used to determine the diameter of the ablated lesion including the tumor with adequate margins.

A previous study reported that complete ablation with RFA was reached in 87% of the cases reviewed², although it was unclear whether complete tumor necrosis was achieved as it is not easy to determine cell death after treatment.^{2,4,5} In fact, one of the major challenges described in the literature involves the determination of tumor cell death after RFAs, especially in the periphery of the ablated tumor area.^{8,9}

In general, cell damage is evaluated by a combination of Hematoxylin and Eosin (H&E) staining and Nicotinamide adenine dinucleotide (NADH) staining, which requires frozen material and poses technical difficulties. Although several studies have shown that evaluation of the therapeutic effects using NADH-diaphorase staining is useful, evaluation of therapeutic effects by RFA would become more reproducible and accurate if evaluations were effectively done using HE-stained sections of formalin-fixed, paraffin-embedded tissues.¹⁰⁻¹⁴ Alternatively, Cytokeratins 8 and 18 (CK8/CK18) immunostaining can be used in paraffin-embedded sections, which are probably easier to standardize.^{4,5,15-18}

Some studies have shown that the CK8^{4,18} and CK18^{15,16} immunostaining of paraffin-embedded sections is comparable to the NADH-diaphorase staining of frozen sections in assessing cell viability, with fewer technical and cost requirements. Thus, CK8/18 could be surrogate markers of tumor cell viability in breast carcinomas subjected to RFAs since they are cleaved at an early step in cell death. Additionally, Cytokeratin 19 (CK19) is a type I keratin that has been described to be cleaved in cell death.

The aim of this study was to evaluate different staining techniques assessing cell death after ultrasound (US)-guided percutaneous radiofrequency ablation (RFA) in the treatment of invasive breast carcinoma.

Methods

An *ex vivo* study was first performed to determine

the optimal methodology to acquire an adequate lesion diameter and avoid adverse effects. This was followed by an *in vivo* experimental study.

The study was approved by the Institutional Review Board (ethical committee) of our hospital (reference AC133/12), and the procedures were performed according to the ethical standards of the World Medical Association (Declaration of Helsinki). A prospective trial was conducted at a Health Insurance Portability and Accountability Act compliant single site. Institutional Review Board approval was obtained, and all participants signed informed consent. The trial was registered at ClinicalTrials.gov with the identifier number NCT02281812.

Ex vivo study

A preliminary RFA was performed on two mastectomy specimens to test the electrode, practice the US technique and evaluate the macroscopic and microscopic effects of the RFA. Under US guidance, electrodes were inserted through the tumour and RF was applied for less than 5 minutes.

In vivo study

The prospective study was conducted at the Multidisciplinary Breast Cancer Unit of Hospital Bellvitge-Institut Catala d'Oncologia. Twenty patients with T1 invasive ductal carcinoma of the breast were treated with RFA *in vivo* followed by immediate surgery from September 2013 to February 2017. These patients had been previously reported¹⁹, publishing the safety and efficacy of the US-guided percutaneous RFA as a local treatment for breast cancer with a reduction in intraoperative margin involvement compared with standard surgical treatment. The present study describes the technical aspects of US-guided percutaneous RFA and evaluates different staining techniques to assess cell death after RFA.

The inclusion criteria were: (1) women, (2) aged > 40 years, (3) invasive ductal carcinoma (not otherwise specified (NOS)) of the breast diagnosed by core needle biopsy, (4) intraductal component less than 20% of the tumor, (5) tumor size ≤ 20 mm, (6) tumor clearly visible by ultrasound and (7) tumor located at least 10 mm from the skin surface and chest wall. The exclusion criteria were: (1) men, (2) aged < 40 years, (3) pregnancy or breast-feeding women, (4) radiological suspicion of multifocal breast cancer, (5) extensive intraductal carcinoma, (6) lobular carcinoma, (7) neoadjuvant therapy and (8) prior surgery or radiotherapy of the ipsilateral breast. Subjects that met all the inclusion criteria and none of the exclusion criteria were included in the study.

Tumour size was measured by US and categorized into two groups: < or ≥ 15 mm.

A Cool-tip™ RF ablation cluster system (Covidien, Tyco Healthcare Group LP, Boulder, CO



80301-3299 USA) was used. This system consists of three 17-gauge straight electrodes, with internally circulating chilled water designed to cool the tissue adjacent to the electrode, limiting tissue charring and maximizing energy deposition.

The *in vivo* procedure was performed in the operating room, under general anaesthesia and sterile conditions. Real-time US was performed using the Flex Focus 400 Ultrasound Machine (BK Ultrasound, BK Medical UK Ltd.). The transducer was covered with a sterile sheath.

Prior to the RFA, at least three additional fresh core needle biopsy specimens from the tumor were obtained for future pathological examination.

All US-guided RFA procedures were performed by two radiologists with 23 and 11 years of experience in breast cancer diagnosis and interventional radiology (AG, AV). The three needle electrodes were guided by US, as parallel to the chest wall as possible. Proper positioning of the 3 electrodes was confirmed in three dimensions to ensure that the expected volume of the thermal lesion was concentric and encompassing the tumour. The tip of the electrodes was placed outside the tumour approximately 5mm from the edge of the tumour. After checking that there was enough safe space between the needle and the skin and the chest wall, RFA was performed for 8 to 10 minutes, using intermittent US monitoring. Two sterile ice packs were placed on the skin overlying the lesion to prevent skin burns during the procedure. The breast was lifted to maximize the distance between the skin and the chest wall. After ablation, the track of the electrode through the tissue was specifically ablated and slowly retracted (track ablation mode) to prevent tumor seeding and to achieve complete hemostasis. The maximum local temperature inside the tumor after the RFA was also recorded and grouped depending on whether or not 70°C was reached.

After RFA, lumpectomy was immediately performed (by A.G.T. and E.F.M., with 19 and 32 years of experience, respectively) with or without the axillary approach according to the National Comprehensive Cancer Network guidelines.²⁰

Pathological evaluation

After lumpectomy the breast specimen was sent to the pathology department. After weighing and inking, the specimen was serially sectioned at 4-mm intervals. The tumour and the ablated area were identified and measured.

One frozen tumour tissue sample of a representative area of the tumour was selected and placed in optimal cutting temperature compound embedding medium, snap frozen in liquid nitrogen and stored at -80°C. Depending on the size of the tumour, 3 to 6 sections were obtained from representative areas of the tumour, adjacent breast tissue and margins and fixed in 10% neutral buffered formalin for 18-72 hours, embedded in paraffin and sectioned.

NADH staining (ref. 107727, Roche) was performed on 8- μ m frozen sections. This staining causes an oxidation reaction in the cytoplasm of viable cells, producing a dark blue stain, with non-viable cells appearing pale gray in color.¹⁴ COX, also referred to as complex IV, is a component of the electron transport chain in the mitochondria, and is involved in the initiation of apoptosis. SDH is the first enzyme in the succinate oxidase chain, which ends in respiratory reactions. Like COX, it is also a marker of mitochondrial activity. Therefore, the histochemical detection of both enzymes reflects cell viability. For COX staining, cells with normal mitochondrial function appear brown, while those with low activity appear blue, and for SDH staining, cells with normal mitochondrial function appear blue, while those with low activity appear pale gray.²¹

H&E-stained slides were prepared from all the blocks submitted and the tissue block containing the most optimally ablated tissue was selected for CK18 (Ref. GAG18, clone DC10, Agilent-DAKO, Dako Omnis) and CK19 (Ref. GA561, clone RCK108, Agilent-DAKO, Dako Omnis) immunostaining. Cytokeratins are intermediate filament keratins found in the intracytoplasmic cytoskeleton of epithelial tissues. CK18 and CK19 are markers for epithelial tumors and apoptosis.^{16,17}

TUNEL assays (Apoptag Plus Peroxidase In situ Apoptosis Kit, Catalogue number S7101, Sigma-Aldrich) are used for the *in situ* detection of DNA degradation in apoptotic and necrotic cells. The labeled cells are visualized on a fluorescent microscope as those with heterogeneously stained (green) nuclei.²²

NADH-diaphorase, SDH and COX activities were scored as diffusely positive if > 50% of the tumor cells showed positive staining, focally positive if less than 50% of the tumor cells showed staining, and negative if there was no staining.

CK18 and CK19 were categorized into five groups according to the percentage of tumor cells that showed a positive staining for them, as follows: negative: less than 10%, 10%–25%, 26%–50%; positive: 51%–75%, and 76%–100%. The final cut-off to consider a complete RFA by cytokeratin staining was below 25%. The TUNEL staining results were categorized as either negative or positive when death cells were detected.

For the control tests, all the staining techniques were also performed on the non-ablated tissue obtained from the core needle biopsies just before the RFA procedure.

The effects of the RFA and cell viability were assessed by three pathologists (T.S., A.P. and C.C., with 35, 13 years of experience and “in training” respectively).

Statistical analysis

Principal component analysis (PCA) for



categorical data was performed as an exploratory analysis to reduce the original set of variables (stains) into a smaller set of uncorrelated components that represented and also summed up the information found in the original variables. PCA is useful in highlighting strong patterns from complex biological datasets. By reducing the dimensionality, a few components rather than several variables are interpreted, and similarities and differences among the variables (e.g., stains) become apparent. We chose the optimal-scaling approach in PCA because it allows variables to be scaled at different levels (e.g., CK18 staining was scaled in five grades and SDH staining in four grades). As a result, nonlinear relationships between the variables can be modeled at different scales. A PCA loading biplot was obtained, on which both the PCA scores of the samples (cases) and loadings of the variables (vectors) were projected. The further away these vectors are from

the origin, the more influence the variable has on the PCA. Loading vectors also indicate how variables correlate with one another: a small angle indicates a positive correlation, while a large angle (e.g., 180°) suggests a negative correlation. The overall internal consistency of the staining methods was assessed using Cronbach's alpha.²³ Categorical variables are described as the number of cases and proportions. Statistical analyses were performed using the SPSS package version 23.0.

Results

From September 2013 to February 2017, a total of 20 patients treated for invasive ductal carcinoma of the breast were recruited for this study (Figure 1). The mean size of the tumors was 11 mm, 15 tumors measuring < 15 mm, and 5 tumors ≥ 15 mm. The overall mean age of the patient sample was 64 years (46–86 years).

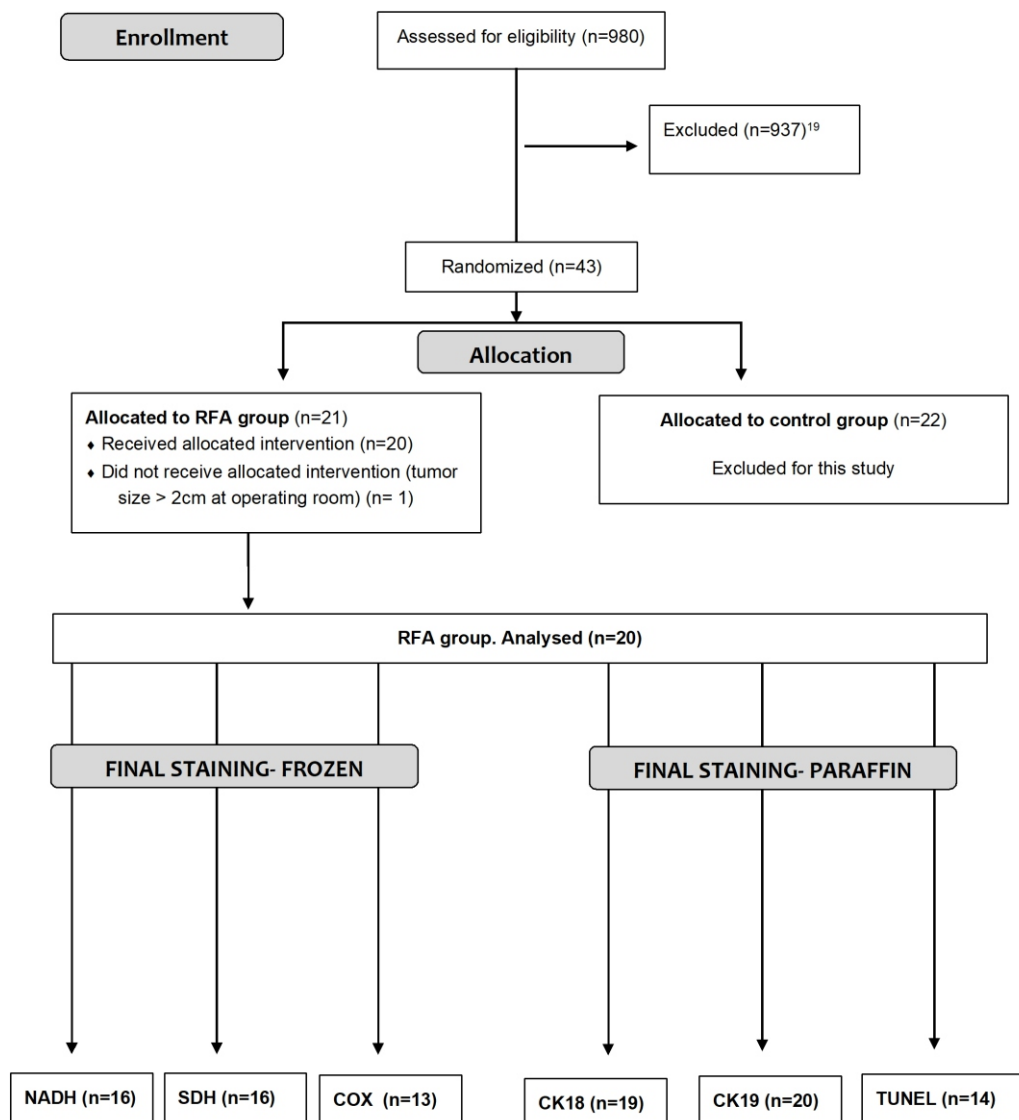


Figure 1. Flow chart shows participants in RFA

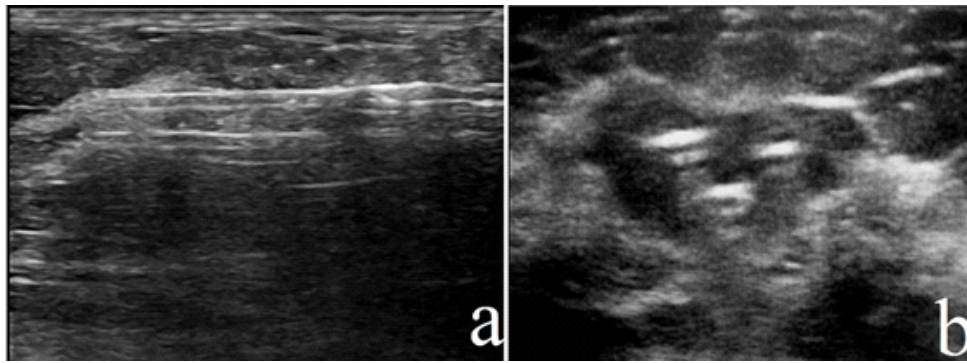


Figure 2. Ultrasound images, transverse (a) and coronal (b) planes with confirmation in three dimensions of correct placement of the 3 electrodes.

Correct placement of the electrodes inside the tumor was achieved in all the cases (Figure 2 a,b). During the ablation treatment, real-time US examination showed that the target lesion and the surrounding tissues became an area of echogenic foci due to tissue heating and microbubble formation. There were no burns to the skin or chest wall.

On gross examination, the ablated area was observed as an ellipsoid central area of necrotic white tumor tissue with central charring and the needle tracks inside. This was surrounded by non-tumor fibro-adipose tissue that looked firm and had changed to a yellowish tan colour. This area was well delineated by a demarcated hyperaemic rim, which represented viable breast tissue (Figure 3 a,b). The median largest ablation diameter was 35 mm (range, 25–60 mm), while the median smallest ablation diameter was 30 mm (range, 20–35 mm).

The criteria for the H&E evaluation of the effects of RFAs on breast cancer have been previously described.⁹ In our series, microscopic changes observed with H&E staining of the frozen and fixed section were similar to the ones reported previously with thermal effects in all the lesions: tissue shrinkage, hyperchromatic neoplastic cells with eosinophilic cytoplasm and pyknotic “streaming” nuclei, and secondary artefactual changes, with degenerative changes in the fibrous connective tissue.

Tumor and the adjacent non-tumoral tissue in the

ablated area exhibited the same behaviour regarding morphology on H&E. Stainings with NADH, COX, SDH, CK18 and CK19 were similar in tumor and adjacent non-tumoral tissue whenever non-tumoral tissue was represented in the slide analyzed. However, non-tumoral tissue located in the periphery of the ablated area did not present any change on H&E and showed a preserved histology. All margins of the tumours were adequately ablated.

Since cell death due to thermal effects is time-dependent, H&E staining alone cannot be used to evaluate cell death in specimens obtained immediately after an RFA, as with this study. Thus, it is better to assess degenerative changes and cell death a few months after an RFA.^{14,24}

Figures 3, 4, 5 and 6 show the microscopic features of the biopsies and ablated tumors treated with the different staining techniques. Frozen sections could not be obtained in 4 of the 20 cases due to technical problems. Thus, NADH and SDH stainings were assessed in 16 of the 20 cases before and after the RFA. All tumors were positive for SDH and NADH before the RFA. After the RFA, however, SDH and NADH positivity was lost in 13 of the 16 tumors (81%). In the three tumors where SDH and NADH positivity was maintained (19%), two were focal and one diffuse. The focal staining occurred around the needle when the track ablation was not feasible. COX staining could only be performed in 13 cases, but their results were comparable with those of NADH staining.

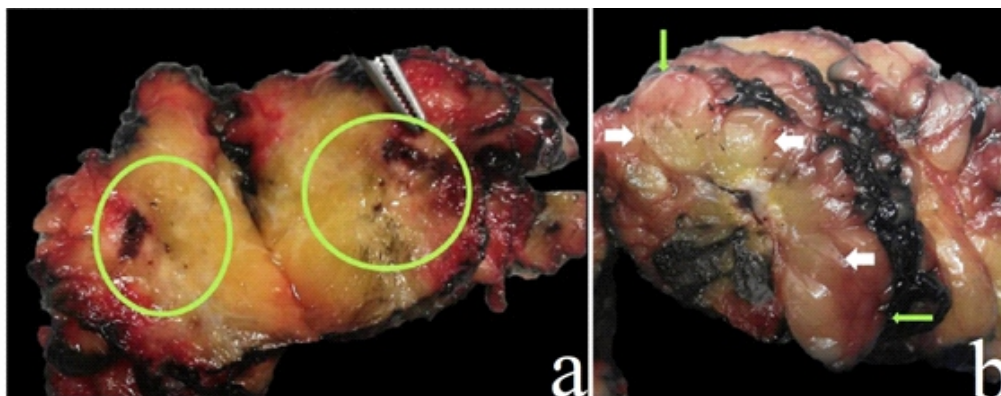


Figure 3. Macroscopic appearance of breast specimen after ablation: central charring of the needle track through the center of the tumor (a) with a surrounding area of yellow, coagulated, adipose and breast tissue (white arrows in b). Red fat is seen in the area outside the zone of thermal destruction (green arrows).

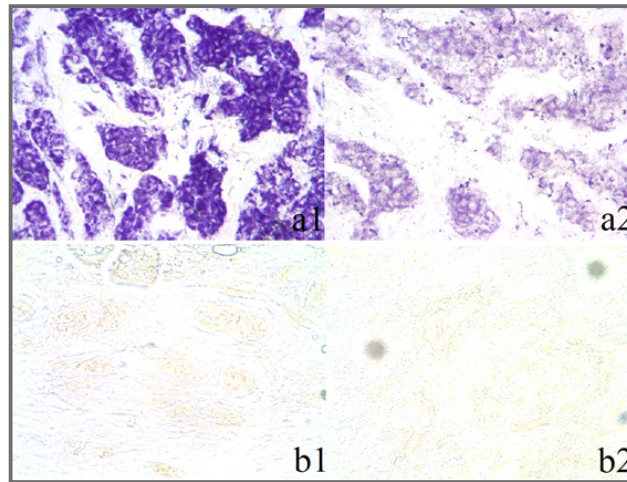


Figure 4. Comparison between NADH and SDH on frozen sections pre (a) and post-radiofrequency (b) (all images, 400x). Pre-radiofrequency diffuse positivity for NADH (a1) and SDH (a2) demonstrates presence of enzymatic activity. Post-radiofrequency negativity for NADH (b1) and SDH (b2) supports absence of viable cells.

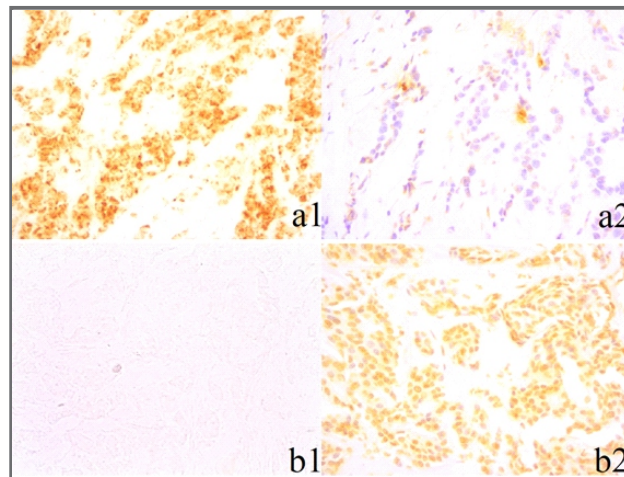


Figure 5. Comparison between COX on frozen sections and TUNEL in paraffine pre (a) and post-radiofrequency (b) (all images, 400x). Pre-radiofrequency section shows diffuse positivity for COX (a1), and absent TUNEL staining (viable) (a2). Post-radiofrequency COX negativity with absence of viable cells (b1), and TUNEL staining with positive nuclear staining in post-ablated tumor (non-viable) (b2)

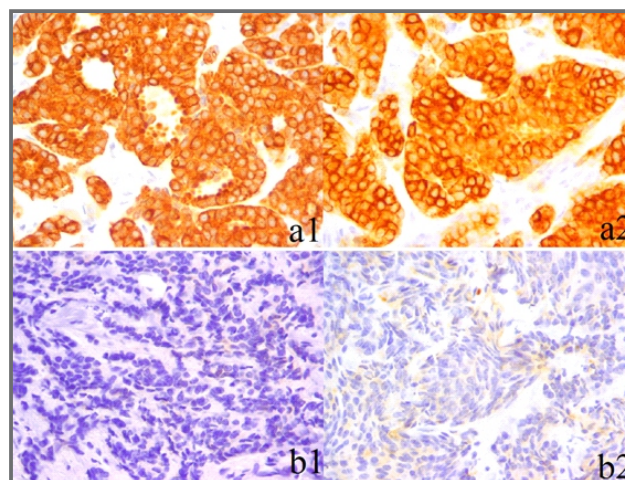


Figure 6. Microscopic features comparing previous biopsy with ablated tumour with Cytokeratin 18 and Cytokeratin 19 pre (a) and after radiofrequency (b) (all images, 400x). Pre-radiofrequency the cells show diffuse immunostaining for Cytokeratin 18 (a1) and 19 (a2). Conversely, post-radiofrequency cytotkeratin 18 (b1) and 19 (b2) expression is reduced with focal positive cells highlighted with cytotkeratin 18 and complete loss with cytotkeratin 19.



Considering the technical difficulties involved in processing frozen tissues, we tried to verify cell death with markers evaluated in paraffin samples. Diffuse CK18 and CK19 staining was found in 19 and 20 tumors, respectively, before the RFA. After the RFA, one case showed CK18 stain between 25-50% of the cells, 6 cases between 10-25%, below 10% in 5 cases and negative in 8. In any case, all tumors showed a lower percentage of positive cells (less than 50%), except one that was still positive for CK18. The TUNEL technique revealed damaged cells in 78% of the tumors assessed, while COX staining indicated a loss of normal mitochondrial function in 84% of the cases studied.

The reliability and internal consistency between the different staining techniques was high, with a Cronbach's alpha of 0.8 (Figure 7). TUNEL staining correlated negatively with the detection of mitochondrial enzymes (COX, NADH and SDH), while the staining results of the mitochondrial enzymes and cytokeratins showed a clear but low internal correlation.

The RFA samples (all of the 20 cases; 100%) showed a complete absence of staining of at least one of the following three: NADH, CK18 or CK19. The results are summarized in Table 1. However, there were 3 cases where > 50% of the tumor cells showed mitochondrial enzyme activity after the RFA. These 3 cases were from patients with tumors measuring > 15mm, in whom the maximum temperature achieved at the center of the tumor after the RFA was ≤ 70°C. Mitochondrial enzyme activity disappeared in the tumors where the temperature after the RFA was > 70°C (p < 0.001).

Discussion

US-guided percutaneous RFA of small invasive breast carcinomas was a feasible and safe technique, as we have demonstrated previously.¹⁹ NADH staining is the standard procedure used for assessing tissue viability following RFA. However, it requires frozen tissue, which is not always available in routine practice, and its accuracy is questionable, especially in the margins of the ablated area, where abundant fatty tissue can make it difficult to obtain a frozen section.^{14, 15, 23, 25} NADH staining was completely absent in 81% of our cases, similar to previous findings. Other studies have found viable invasive tumor cells in around 15-21% of RFA cases at the margins of the tumor or lining the needle track.^{12, 18, 26} By contrast, one study did not find viable tumor tissues in any of the 23 RFA cases evaluated with NADH staining, both immediately after the RFA and a period after the procedure.²⁷

COX and SDH staining are techniques described in RFAs in hepatic tissues.^{28, 29} In our series, SDH and COX staining was absent in 81% and 84% of the cases, respectively, which was in perfect concordance with the results of NADH staining.

The TUNEL technique performed on paraffin sections has been described for RFAs in skin tissues³⁰ and hepatocellular carcinoma.²⁷ In our series, cell death was confirmed by the TUNEL technique in 11 of the 12 cases studied, whose results were also consistent with those of the other staining techniques.

In this study, CK19 showed absence or reduction of expression in all tumors after the RFA, while CK18 in all tumors except one. CK18 and CK19

Table 1. Results of pathologic stainings

Patient	NADH pre	NADH post	SDH pre	SDH post	COX pre	COX post	Ck18 pre	Ck18 post	Ck19 pre	Ck19 post	TUNNEL pre	TUNNEL post
1	2	0	2	0	2	0	4	2	4	0	1	0
2	2	0	2	0	2	0	4	2	4	2	1	0
3	2	0	2	0	2	0	4	0	4	0	1	0
4	2	0	2	0	2	0	0	0	0	0	1	0
5	N/A	N/A	N/A	N/A	N/A	N/A	4	1	4	0	1	0
6	N/A	N/A	N/A	N/A	N/A	N/A	4	0	4	0	0	0
7	N/A	N/A	N/A	N/A	N/A	N/A	4	0	4	0	1	0
8	2	0	2	0	N/A	N/A	4	0	4	0	1	0
9	2	1	2	1	2	1	4	1	4	1	1	0
10	2	2	2	2	2	1	4	2	4	2	1	0
11	2	1	2	1	1	0	4	3	4	2	1	1
12	2	0	2	0	2	0	4	0	4	0	1	0
13	2	0	1	0	N/A	N/A	4	2	4	2	1	1
14	2	0	2	0	N/A	N/A	4	1	4	0	1	0
15	2	0	2	0	2	0	4	1	4	1	N/A	N/A
16	2	0	2	0	2	0	4	2	4	2	N/A	N/A
17	2	0	2	0	2	0	4	0	4	0	N/A	N/A
18	2	0	2	0	2	0	4	2	4	2	N/A	N/A
19	N/A	N/A	N/A	N/A	N/A	N/A	4	1	4	1	N/A	N/A
20	2	0	2	0	2	0	4	0	4	1	N/A	N/A

N/A not available

NADH-diaphorase, SDH and COX: 2: >50% diffusely positive; 1: <50% focally positive, 0: negative

CK18 and CK19: 0: less than 10%, 1: 10%–25%, 2: 26%–50%, 3: 51%–75%, 4: 76%–100%.

Tunnel: 0: negative, 1: positive.

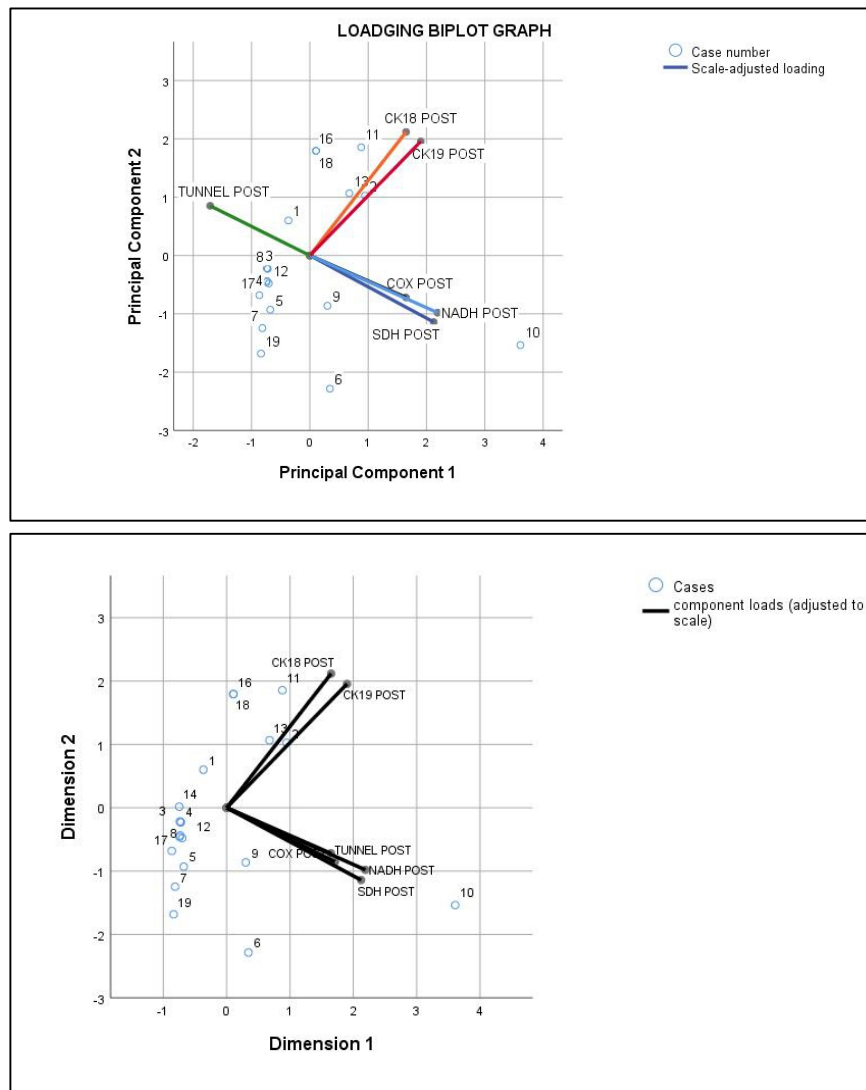


Figure 7. Biplot of staining results: In this graph, both PCA scores of samples (cases) and loading of variables (vectors) are pictured. The further away these vectors are from the origin, the more influence the variable has on PCA. Loading vectors also hint at how variables correlate with one another: a small angle implies positive correlation; a large angle (eg. 180°) suggests negative correlation. Note (a) the negative correlation (180° angle between vectors) between TUNEL staining (which stains apoptosis) and Cox, NADH and SDH (which assess mitochondrial activity). Note also the perfect correlation among mitochondrial enzymes themselves and also along cytokeratins themselves (b). However, correlation between cytokeratins and the rest of enzymes is weak likely because more than 50% of the cases presented residual staining.

staining could be performed in all the cases, except for one in the case of CK18 staining, which was negative in the control sample. It should be noted that approximately 5% to 15% of breast carcinomas may not express CK18/19. Thus, core needle biopsies should be analyzed to confirm the presence of cytokeratins before ablation.¹⁵ Therefore, correlation of cytokeratin staining results with those of other markers of viability is necessary.

The reliability and internal consistency between the staining techniques was high, with the NADH-SDH-COX staining results correlating strongly with the TUNEL results and the CK18 staining results correlating clearly with those of CK19. However, due to high sensitivity in detecting residual cytokeratin activity, there is no strong correlation between mitochondrial enzyme and cytokeratin

staining techniques. That is why the cut-off to consider complete ablation was different between mitochondrial enzyme and cytokeratin staining; therefore, the final result could be considered acceptable with both techniques. It is likely that the residual staining of cytokeratins after immediate death may account for this different behaviour with mitochondrial enzymes. In any case, CK18 and CK19 staining techniques are simple, reproducible, and show good concordance. Thus, they can be used as markers of cell viability. As these techniques can be performed on fixed sections, CK18 and CK19 assessment is simpler and more economical than those using frozen sections. Provided that there is good concordance between a loss of enzymatic activity and the loss of CK18 and CK19 expression, CK18 and CK19 could be considered surrogate



markers of cell viability.

To our knowledge, this study is the first to assess COX, SDH, TUNEL and CK19 staining in the evaluation of cell viability after a RFA in breast cancer, allowing us to compare the techniques and the causes of persistent tumor cell viability. The limitations of this study were the small number of cases and the surgical excision being performed immediately after the RFA that could have led to an underestimation of tumor necrosis.

We observed an absence of cellular viability in at least one of the markers in all our cases, although the possibility of viable cells remaining in the tumor after an RFA cannot be completely ruled out. The specificity of any of the staining techniques in ruling out any remaining non-necrotic tumor tissue was high after the complete inclusion of the resection specimen, although we did perform the assessments immediately after the RFA.

In conclusion, US-guided percutaneous RFA of small invasive breast carcinoma is a feasible and safe technique that could be an option for less invasive treatments. Staining techniques assessing cell viability revealed decreased NADH, COX and SDH staining in frozen sections and positive TUNEL results. CK18 and CK19 staining results in paraffin-embedded sections showed an excellent correlation with those of the other markers studied in frozen sections, becoming negative after the RFA. Thus, CK18 and CK19 immunohistochemistry can be used to assess RFA efficacy in paraffin-embedded tissues, which is simpler and more economical than the methods using frozen tissues.

Acknowledgment

We thank Griselda Ventura, MSc, for the technical support on immunohistochemical and enzymohistochemical studies and Michael Maudsley, MSc, for language revision.

Conflicts of Interest

The authors declare that they have no conflict of interests.

References

1. Fleming MM, Holbrook AI, Newell MS. Update on image-guided percutaneous ablation of breast cancer. *American Journal of Roentgenology*. 2017;208(2):267-74.
2. Peek MC, Ahmed M, Napoli A, Usiskin S, Baker R, Douek M. Minimally invasive ablative techniques in the treatment of breast cancer: a systematic review and meta-analysis. *International Journal of Hyperthermia*. 2017;33(2):191-202.
3. Chen J, Zhang C, Li F, Xu L, Zhu H, Wang S, et al. A meta-analysis of clinical trials assessing the effect of radiofrequency ablation for breast cancer. *OncoTargets and therapy*. 2016;9:1759.
4. Schässburger K-U, Löfgren L, Lagerstedt U,

- Leifland K, Thorneman K, Sandstedt B, et al. Minimally-invasive treatment of early stage breast cancer: a feasibility study using radiofrequency ablation under local anesthesia. *The Breast*. 2014;23(2):152-8.
5. Waaijer L, Krebs D, Gallardo MF, Van Rossum P, Postma E, Koelemij R, et al. Radiofrequency ablation of small breast tumours: evaluation of a novel bipolar cool-tip application. *European Journal of Surgical Oncology (EJSO)*. 2014;40(10):1222-9.
6. Organ L. Electrophysiologic principles of radiofrequency lesion making. *Stereotactic and Functional Neurosurgery*. 1976;39(2):69-76.
7. Jeffrey SS, Birdwell RL, Ikeda DM, Daniel BL, Nowels KW, Dirbas FM, et al. Radiofrequency ablation of breast cancer: first report of an emerging technology. *Archives of Surgery*. 1999;134(10):1064-8.
8. Earashi M, Noguchi M, Motoyoshi A, Fujii H. Radiofrequency ablation therapy for small breast cancer followed by immediate surgical resection or delayed mammotome excision. *Breast Cancer*. 2007;14(1):39-47.
9. Seki K, Tsuda H, Iwamoto E, Kinoshita T. Histopathological effect of radiofrequency ablation therapy for primary breast cancer, with special reference to changes in cancer cells and stromal structure and a comparison with enzyme histochemistry. *Breast cancer*. 2011;18(1):18-23.
10. Manenti G, Scarano AL, Pistolese CA, Perretta T, Bonanno E, Orlandi A, et al. Subclinical breast cancer: minimally invasive approaches. Our experience with percutaneous radiofrequency ablation vs. cryotherapy. *Breast care*. 2013;8(5):356-60.
11. Noguchi M, Motoyoshi A, Earashi M, Fujii H. Long-term outcome of breast cancer patients treated with radiofrequency ablation. *European Journal of Surgical Oncology (EJSO)*. 2012;38(11):1036-42.
12. Tsuda H, Seki K, Hasebe T, Sasajima Y, Shibata T, Iwamoto E, et al. A histopathological study for evaluation of therapeutic effects of radiofrequency ablation in patients with breast cancer. *Breast Cancer*. 2011;18(1):24-32.
13. Yamamoto N, Fujimoto H, Nakamura R, Arai M, Yoshii A, Kaji S, et al. Pilot study of radiofrequency ablation therapy without surgical excision for T1 breast cancer: evaluation with MRI and vacuum-assisted core needle biopsy and safety management. *Breast Cancer*. 2011;18(1):3-9.
14. Yoshinaga Y, Enomoto Y, Fujimitsu R, Shimakura M, Nabeshima K, Iwasaki A. Image and pathological changes after radiofrequency ablation of invasive breast cancer: a pilot study of nonsurgical therapy of early breast cancer. *World journal of surgery*. 2013;37(2):356-63.



15. Bloom KJ, Dowlath K, Assad L. Pathologic changes after interstitial laser therapy of infiltrating breast carcinoma. *The American journal of surgery*. 2001;182(4):384-8.
16. Burak Jr WE, Agnese DM, Povoski SP, Yanssens TL, Bloom KJ, Wakely PE, et al. Radiofrequency ablation of invasive breast carcinoma followed by delayed surgical excision. *Cancer: Interdisciplinary International Journal of the American Cancer Society*. 2003;98(7):1369-76.
17. Duan WR, Garner DS, Williams SD, Funckes-Shippy CL, Spath IS, Blomme EA. Comparison of immunohistochemistry for activated caspase-3 and cleaved cytokeratin 18 with the TUNEL method for quantification of apoptosis in histological sections of PC-3 subcutaneous xenografts. *The Journal of Pathology: A Journal of the Pathological Society of Great Britain and Ireland*. 2003;199(2):221-8.
18. Kreb D, Bosscha K, Ernst M, Rutten M, Jager G, Van Diest P, et al. Use of cytokeratin 8 immunohistochemistry for assessing cell death after radiofrequency ablation of breast cancers. *Biotechnic & Histochemistry*. 2011;86(6):404-12.
19. García-Tejedor A, Guma A, Soler T, Valdivieso A, Petit A, Contreras N, et al. Radiofrequency ablation followed by surgical excision versus lumpectomy for early stage breast cancer: a randomized phase II clinical trial. *Radiology*. 2018;289(2):317-24.
20. Gradishar WJ, Anderson BO, Balassanian R, Blair SL, Burstein HJ, Cyr A, et al. NCCN guidelines insights: breast cancer, version 1.2017. *Journal of the National Comprehensive Cancer Network*. 2017;15(4):433-51.
21. Simard ML, Mourier A, Greaves LC, Taylor RW, Stewart JB. A novel histochemistry assay to assess and quantify focal cytochrome c oxidase deficiency. *The Journal of pathology*. 2018;245(3):311-23.
22. Kabakov AE, Gabai VL. Cell death and survival assays. *Chaperones: Springer*; 2018. p. 107-27.
23. Singla K, Sandhu SV, Pal RA, Bansal H, Bhullar RK, Kaur P. Comparative evaluation of different histoprocessing methods. *International journal of health sciences*. 2017;11(2):28.
24. Oura S, Tamaki T, Hirai I, Yoshimasu T, Ohta F, Nakamura R, et al. Radiofrequency ablation therapy in patients with breast cancers two centimeters or less in size. *Breast cancer*. 2007;14(1):48-54.
25. Fornage BD, Sneige N, Ross MI, Mirza AN, Kuerer HM, Edeiken BS, et al. Small (≤ 2 -cm) breast cancer treated with US-guided radiofrequency ablation: feasibility study. *Radiology*. 2004;231(1):215-24.
26. Kreb D, Looij B, Ernst M, Rutten M, Jager G, van der Linden J, et al. Ultrasound-guided radiofrequency ablation of early breast cancer in a resection specimen: lessons for further research. *The Breast*. 2013;22(4):543-7.
27. Motoyoshi A, Noguchi M, Earashi M, Zen Y, Fujii H. Histopathological and immunohistochemical evaluations of breast cancer treated with radiofrequency ablation. *Journal of surgical oncology*. 2010;102(5):385-91.
28. Ishizaka H, Ishijima H, Katsuya T, Koyama Y. Percutaneous ethanol injection therapy: use of a directable needle guide. *American journal of roentgenology*. 1997;168(6):1563-4.
29. Itoh T, Orba Y, Takei H, Ishida Y, Saitoh M, Nakamura H, et al. Immunohistochemical detection of hepatocellular carcinoma in the setting of ongoing necrosis after radiofrequency ablation. *Modern pathology*. 2002;15(2):110-5.
30. Lee JM, Park JH, Kim BY, Kim I-H. Terminal deoxynucleotidyl transferase-mediated deoxyuridine triphosphate nick end labeling (TUNEL) assay to characterize histopathologic changes following thermal injury. *Annals of dermatology*. 2018;30(1):41.